Molecular Crystals and Liquid Crystals
Publication details, including instructions for authors and subscription information:
http://www.tandfonline.com/loi/gmcl16

Structural Analysis of the Intermediate Phases of $(n\text{-}C_{13}H_{27}NH_3)_2ZnCl_4$ by Single Crystal Diffraction

F. J. Zuñiga [a b] & G. Chapuis [a]
[a] Institut de Criostallographie, Université de Lausanne, 1015 Lausanne, Swiotzerland
[b] Departmento de Fisica, Universidad del Pais Vasco, Spain
Version of record first published: 20 Apr 2011.

To cite this article: F. J. Zuñiga & G. Chapuis (1985): Structural Analysis of the Intermediate Phases of $(n\text{-}C_{13}H_{27}NH_3)_2ZnCl_4$ by Single Crystal Diffraction, Molecular Crystals and Liquid Crystals, 128:3-4, 349-366

To link to this article: http://dx.doi.org/10.1080/00268948508079501

Mol. Cryst. Liq. Cryst., 1985, Vol. 128, pp. 349–366
0026-8941/85/1284–0349/$20.00/0

Printed in the United States of America

Structural Analysis of the Intermediate Phases of (n-$C_{13}H_{27}NH_3)_2ZnCl_4$ by Single Crystal Diffraction

F. J. ZUÑIGA† and G. CHAPUIS

Institut de Cristallographie, Université de Lausanne, 1015 Lausanne, Switzerland

(*Received March 19, 1984; in final form December 3, 1984*)

The structure of (n-$C_{13}H_{27}NH_3)_2ZnCl_4$ consists of two-dimensional layers of alkylammonium chains stacked alternately with layers of isolated $ZnCl_4$ tetrahedra. Consecutive layers are linked by H-bonds between the N and Cl atoms. In the temperature range from 20 to 50°C, five different phases could be identified, four of which were analyzed by single crystal diffraction. In each phase, all the chains are essentially parallel. In the room temperature phase, the direction of the chains is inclined with respect to the normal to the layer whereas it is nearly parallel to the normal in the other phases. The phase which is stable directly above room temperature is characterized by the total disappearance of the kinks observed in the room temperature phase. They reappear in the phases stable at higher temperatures but at varying positions and on varying chains depending on the phase. All the transitions but one have a first order character and are reversible. The room temperature phase of an untreated sample cannot be recovered after a heating cycle and must therefore be considered metastable.

1. INTRODUCTION

Compounds of the type $(C_nH_{2n+1}NH_3)_2MX_4$ with M = Cu, Mn, Cd, Fe, Zn, Co, X = Cl, Br and $n \geq 5$ exhibit several solid-solid phase transitions resulting from the dynamics of the hydrocarbon chains. With increasing temperature, the various phases observed in each compound reach a quasi-liquid state involving partial melting of the aliphatic entities. This state is preceded by a series of transitions,

†Present address: Departamento de Fisica, Universidad del Pais Vasco, Spain.

depending on the number n of carbon atoms in the organic chains and the cation M (M = Zn[1]; Cu[2] and Cd[2]). On the basis of calorimetric, NMR, dielectric, optical and X-ray diffraction studies on some members of this family, it has been established that the transitions result from the combination of two types of mechanisms: order-disorder transformations of rigid chains and cooperative conformational changes of the alkylammonium chains.[3]

For M = Cd and n = 10, the first pre-transition is associated with a specific change in the conformation of the chains,[2] whereas in the main transition the chains change to a quasi-liquid state. A dynamic model based on "kinks" moving along the chains has been proposed for this transition.[3-4] A dynamical approach for the phase transitions in $(C_{14}H_{29}NH_3)_2ZnCl_4$ has also been published.[5] In a pre-transition at 362.5 K, the symmetry of the crystal changes from monoclinic to orthorhombic as a result of orientational disordering of the chains. The transition at 367 K is due to a cooperative melting of the chains.

No structural studies have been published for the phases preceding the melting of the chains. In almost all cases the pre-transitions occur in a narrow temperature range and sometimes overlap with the last transition, thus making an X-ray analysis difficult or impossible. For M = Zn and n = 13 (hereafter C13Zn), the series of pre-transitions are sufficiently resolved in temperature to allow X-ray measurements of the intermediate phases.

From the structural point of view, compounds with M = Zn and Co differ from those with M = Cu, Cd, Mn and Fe. The first group consists of layers of isolated MX_4 tetrahedra alternating with organic layers of intercalated chains.[6] The second group consists of bidimensional networks of corner sharing MX_4 octahedra alternating with layers of non-intercalated chains.[3] In this group the organic layer is very similar to the structure of lipid bilayers. The difference in the packing of the aliphatic part is relevant since it governs the sequence of phase transitions.

In the Zn derivatives, the sequence of transitions depends on the parity of n and has been correlated with packing characteristics.[7] For odd values of n, two pre-transitions have been reported whereas for even values of n, only one is mentioned.[1] In this work, the structural characteristics of the high temperature phases observed for C13Zn will be described. The structures of the phases observed between 293 and 333 K have been studied with the aim to understand the transition mechanisms. The structures include the intermediate phase IV and a new room-temperature phase V′ obtained by cooling phase IV. Preliminary results for the intermediate phases III and II are also

available. The structure of the room temperature phase V has already been reported.[7]

We also report a differential scanning calorimetric (DSC) analysis showing some discrepancies between the thermal behaviour observed by X-ray diffraction and that published for earlier calorimetric studies. In particular, a new intermediate phase has been found which had not been previously described.

2. EXPERIMENTAL

The compound was obtained by spontaneous reaction at room temperature of a stoichiometric mixture of $ZnCl_2$ and $C_{13}H_{27}NH_3Cl$ in ethanol. Single crystals were grown by slow evaporation from the solution. Details on the synthesis have been published elsewhere.[8]

2.1 Calorimetry

Two pre-transitions at 310 and 315.5 K respectively have been reported.[1] Thermal hysteresis and some differences between heating and cooling cycles were attributed to the dynamic nature of the process. In our measurements (Mettler DSC 30), three peaks were observed on heating between room temperature and 333 K. The first two peaks corresponded to the reported pre-transitions. On heating, the two peaks were not completely resolved and a single value of the thermodynamic magnitudes associated with both transitions was calculated. The third peak was weak and not always observed. On cooling, an important thermal hysteresis was observed in the first peak whereas the third peak was not seen anymore. Table I gives the transition temperatures obtained with a scanning rate of 1 K/min and

TABLE I

Transition temperatures and values of the thermodynamic functions of $(C_{13}H_{27}NH_3)_2ZnCl_4$. Cycles were run at a temperature rate of 1 K/min.

	Peak No.	$T(K)$	ΔH(kJ/mol)	ΔS(J/mol.K)
Heating	1	308.0	10.3	33.5
	2	311.5		
	3	320.5	0.95	2.9
Cooling	1	301.7	6.4	21.2
	2	309.0	1.7	5.2
	3	—	—	—

thermodynamic magnitudes averaged over several cycles. It must be noted that the value of ΔH associated with the two peaks in the heating process is greater than the sum of the ΔH corresponding to the individual peaks on cooling. As the enthalpy of the second transition seems to be identical in both processes (see Figure 1), the difference must be associated with the first transition. Previously published values of the transition enthalpies are lower but the same thermal hysteresis had been reported. Other Zn-compounds with n = 11 and 15 exhibit the same characteristics.

2.2 X-ray diffraction

The thermal behaviour of X-ray powder diagrams was studied with a temperature-controlled Guinier camera fitted with a moving film. Exposures were taken in steps of 1 degree and the temperature stability was controlled by a thermocouple. No variations larger than ± 0.2 K were observed during the exposure. Single crystal diffractograms were obtained from a Weissenberg camera with a heating device.

Three discontinuities in the powder diagram were detected on heating between room temperature and 323 K. The transition temperatures were similar to, but not exactly the same as those determined by DSC. The sequence of space group symmetries was established by single-crystal diffractometry where the complete symbols given (see below) indicate the various orientations of the unique axis in the monoclinic system. The last transition at 369 K corresponds to the melting of the chains; the space group symmetry of phase I (*Pnma*) was postulated on the assumption that the chains are statistically distributed between two equivalent positions. The non-centrosymmetric space groups of phases III and II are tentative and must still be confirmed by the full resolution of the structures.[13] Packing considerations are however highly in favor of the non-centrosymmetric space group for phase III.

V	IV	III	II	I	phase
304	309	316	369		transition temp. (K)
$P12_11$	$P112_1/a$	$P2_111$	$Pn2_1a$	*Pnma*	space groups

Transition from the room-temperature phase V to phase IV is observed on the powder diagram as a discontinuity in the diffraction

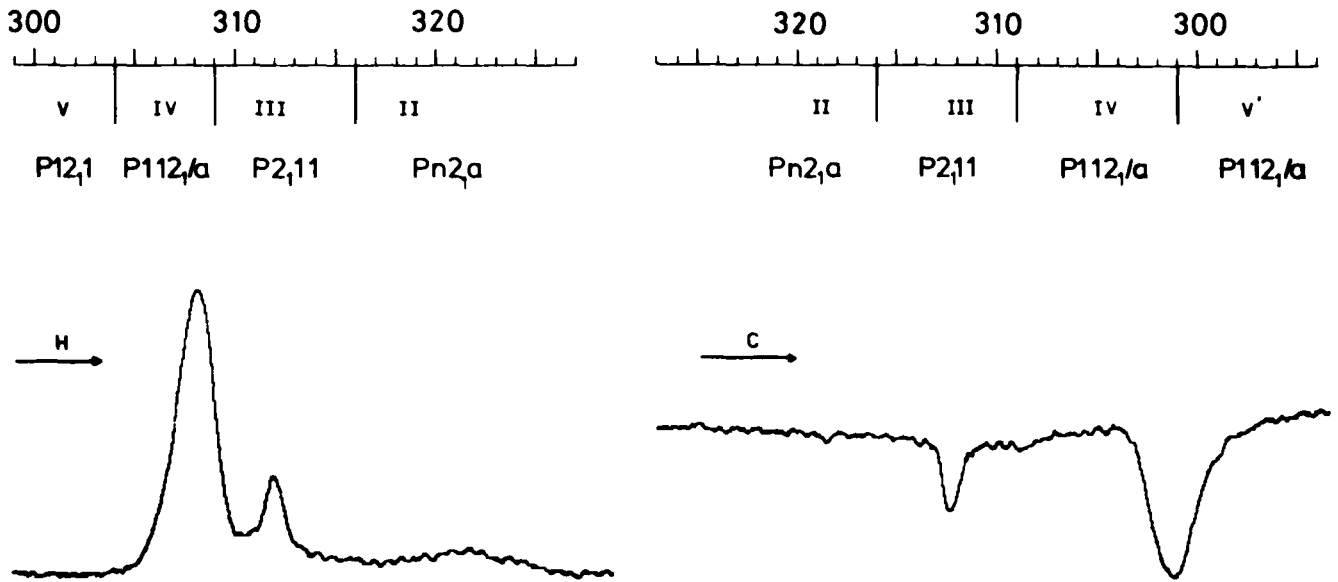

FIGURE 1 Comparison between DSC and X-ray powder diffraction measurements. Temperatures are given in Kelvin; DSC curves are reported on an arbitrary scale. Vertical lines indicate the transition temperatures as found by X-ray.

lines. With increasing temperature, phase V shows an increase of the monoclinic angle β up to a value of 100° at 304 K. Beyond this temperature, the next phase appears with the new axes $\mathbf{a}' = \mathbf{a}$, $\mathbf{b}' = \mathbf{b}$ and $\mathbf{c}' = \mathbf{a} + \mathbf{c}$ and a monoclinic angle $\gamma = 89.35°$. The cell parameters of phase IV do not change significantly in the temperature range where the phase is stable. On cooling, phase V cannot be observed. Instead, a new room temperature phase V′ appears with space group symmetry $P112_1/a$. Single crystal diffractograms show the same irreversibility and confirm the existence of the new phase V′.

The IV to III phase transition is also observed as a discontinuity on the powder diffractogram. Phase III is monoclinic, but with α as the monoclinic angle. With increasing temperature, the diffraction lines shift continuously up to the next transition. Single crystal diffractograms for phase III reveal the existence of two domains separated by an angle of $2(\alpha - 90°)$. Its value is approximately 7 degrees at 309 K and decreases continuously up to 316 K. Reversibility is observed on cooling from III to IV.

The last intermediate phase II is orthorhombic and stable up to 369 K. At this temperature, the powder diagram changes dramatically with an increase of c by 19%. The cell parameters of phase I obtained by indexing the corresponding powder diffractogram are $a = 10.3$, $b = 7.2$ and $c = 54.1$ Å.

The sequence of transitions found by X-ray diffraction and calorimetry is indicated in Figure 1. In the heating process (H) the agreement is good between both methods; on cooling (C) however, transition II to III is missing on the DSC plot and the transition temperature of III to IV cannot be matched.

Two crystals were used for the structure determination of phases IV, III, II and V′. The Bragg intensities were measured on an automatic four-circle diffractometer (Syntex $P2_1$) equipped with a high-temperature system. A U-shaped heating device was fixed on the χ-circle and the temperature controlled by a thermocouple positioned at a distance of 1.5 mm from the crystal. The apparatus including heating device and crystal was enclosed in a Mylar cylinder mounted parallel to the ϕ-axis. The temperature stability was better than ± 0.2 degrees. Crystal data are given in Table II for each phase along with the experimental specifications for the intensity measurements of phases V′ and IV. With crystal 1, the phases were measured in the order from IV to II; after cooling to room temperature phase V′ was measured six months later. This time interval was introduced to be sure that the single crystal would not revert to phase V.

TABLE II

Crystal data and experimental details for phases V′, IV, III and II.

	V[a]	V′	IV	III	II	I
Temperature	293	293	305	309	318	<362
a (Å)	10.644(2)	10.271(1)	10.2680(9)	10.292(2)	10.316(1)	10.3
b (Å)	7.3074(9)	7.413(1)	7.416(1) 7.452(2)	7.479(1)	7.2	
c (Å)	44.043(7)	45.411(6)	45.428(9)	45.47(1)	45.32(1)	54.1
Monoclinic angle (°)	β = 94.24(2)	γ = 89.46(1)	γ = 89.35(1)	α = 93.42(2)		
V (Å^3)	3416.3	3457.4	3459.0	3481.2	3496.6	4012
Crystal no	—	1	1	2	1	
Space group	$P2_1$	$P2_1/a$	$P2_1/a$	$P2_1$	$Pn2_1a$	
D_x (gr/cm^3)	1.18	1.17	1.17	1.16	1.15	1.01
Z	4	4	4	4	4	4
Wavelength (Å)	1.5418	1.5418	1.5418	1.5418	1.5418	1.54
μ (cm^{-1})		39.2	39.2			
Independent reflect.		2805	1518			
Observed reflect. $I > 3\sigma$ (I)		2232	1238			
$(\sin\theta/\lambda)_{max}$		.4590	.3811			
Measurement method		θ-2θ scan	θ-2θ scan			
Absorption correction by Gaussian integration		yes	yes			
Transmission max./min.		.5646/.4817	.5618/.4735			
R =		0.079	0.072			
R_w =		0.085	0.075			
Goodness-of-fit		5.277	3.804			

[a] From reference 7

TABLE III

Atomic parameters of phase IV. Chain $N(1)$ corresponds to chains $N(1)$ and $N(3)$ of phase V; chain $N(2)$ corresponds to chains $N(2)$ and $N(4)$. $U_{eq} = \frac{1}{3}(U_{11} + U_{22} + U_{33})$

Atom	x	y	z	U_{eq}
Zn	0.2699(2)	0.2531(3)	−0.01553(5)	0.0996(1)
Cl(1)	0.2466(4)	0.2964(6)	0.03353(9)	0.124(2)
Cl(2)	0.4814(4)	0.2416(7)	−0.0276(1)	0.133(2)
Cl(3)	0.1683(4)	0.0003(5)	−0.0295(1)	0.119(2)
Cl(4)	0.1699(4)	0.4919(6)	−0.0366(1)	0.125(2)
N(1)	0.110(1)	0.724(2)	0.0261(3)	0.122(7)
C(11)	0.177(2)	0.801(3)	0.0504(5)	0.144(7)
C(12)	0.149(2)	0.720(2)	0.0793(4)	0.137(6)
C(13)	0.231(2)	0.798(3)	0.1051(4)	0.146(7)
C(14)	0.184(2)	0.719(3)	0.1343(5)	0.152(7)
C(15)	0.254(2)	0.796(3)	0.1615(4)	0.149(7)
C(16)	0.198(2)	0.721(3)	0.1901(4)	0.145(7)
C(17)	0.263(2)	0.796(3)	0.2181(4)	0.145(7)
C(18)	0.201(2)	0.724(2)	0.2455(5)	0.145(7)
C(19)	0.261(2)	0.795(3)	0.2740(4)	0.145(7)
C(110)	0.199(2)	0.727(3)	0.3015(5)	0.153(7)
C(111)	0.258(2)	0.791(3)	0.3303(5)	0.145(7)
C(112)	0.192(2)	0.723(3)	0.3578(5)	0.162(8)
C(113)	0.255(2)	0.783(3)	0.3863(5)	0.179(8)
N(2)	0.063(1)	0.264(2)	0.4583(3)	0.120(7)
C(21)	0.060(2)	0.196(4)	0.4264(6)	0.20(1)
C(22)	0.006(3)	0.305(4)	0.4068(7)	0.22(1)
C(23)	0.014(2)	0.221(4)	0.3723(7)	0.21(1)
C(24)	−0.035(2)	0.285(3)	0.3458(7)	0.20(1)
C(25)	−0.004(2)	0.230(3)	0.3142(6)	0.187(9)
C(26)	−0.047(2)	0.289(4)	0.2867(7)	0.20(1)
C(27)	−0.008(2)	0.233(3)	0.2586(6)	0.180(9)
C(28)	−0.048(2)	0.291(3)	0.2298(7)	0.20(1)
C(29)	−0.003(2)	0.233(3)	0.2034(7)	0.190(9)
C(210)	−0.046(2)	0.289(4)	0.1741(7)	0.21(1)
C(211)	0.001(2)	0.232(3)	0.1484(6)	0.185(9)
C(212)	−0.050(3)	0.292(5)	0.1196(9)	0.28(2)
C(213)	−0.004(2)	0.235(4)	0.0969(6)	0.20(1)

3. DESCRIPTION OF THE STRUCTURES

For the reduction of intensities and refinement of the various phases, the XRAY System[9] of programs was used. Atomic scattering factors for Zn^{2+}, Cl^-, N and C and anomalous dispersion terms for Zn and Cl were used for the structure factor calculations.[10-11] Hydrogen atoms were not included in the models.

Atomic coordinates of Zn and Cl atoms in phase V[7] were used as starting parameters in phase IV after suitable transformation. Atomic

TABLE IV

Atomic parameters and population parameter for the disordered chain of phase V'.

Atom	x	y	z	U_{eq}	p
Zn	0.2702(1)	0.2536(2)	−0.01552(4)	0.0844(6)	
Cl(1)	0.2472(3)	0.2973(5)	0.03370(8)	0.111(2)	
Cl(2)	0.4825(3)	0.2417(6)	−0.02761(8)	0.119(2)	
Cl(3)	0.1682(3)	−0.0005(5)	−0.03002(8)	0.103(2)	
N(1)	0.1705(3)	0.4921(5)	−0.03662(8)	0.107(2)	
C(11)	0.1114(8)	0.728(1)	0.0266(2)	0.105(4)	
C(12)	0.178(1)	0.809(2)	0.0510(3)	0.120(6)	
C(13)	0.151(1)	0.726(2)	0.0795(3)	0.111(6)	
C(14)	0.226(1)	0.796(2)	0.1050(3)	0.124(6)	
C(15)	0.185(1)	0.721(2)	0.1346(3)	0.133(7)	
C(16)	0.249(1)	0.795(2)	0.1606(3)	0.122(7)	
C(17)	0.201(1)	0.728(2)	0.1896(4)	0.130(7)	
C(18)	0.261(1)	0.794(2)	0.2173(3)	0.122(6)	
C(19)	0.207(1)	0.731(2)	0.2451(4)	0.127(7)	
C(110)	0.262(1)	0.792(2)	0.2747(3)	0.123(6)	
C(111)	0.199(1)	0.728(2)	0.3019(4)	0.133(7)	
C(112)	0.256(1)	0.791(2)	0.3309(3)	0.123(6)	
C(113)	0.194(1)	0.728(2)	0.3577(4)	0.147(7)	
N(2)	0.253(1)	0.784(2)	0.3862(4)	0.160(8)	
C(21)	0.0644(7)	0.256(1)	0.4580(2)	0.102(4)	
C(22)	0.060(1)	0.195(3)	0.4271(4)	0.17(1)	
C(23)	0.010(2)	0.295(3)	0.4079(5)	0.21(1)	
C(23)'	0.028(3)	0.219(5)	0.374(1)	0.14(1)	0.54(2)
C(24)	−0.045(4)	0.345(7)	0.383(1)	0.23(2)	0.46
C(24)'	−0.026(2)	0.280(4)	0.3518(7)	0.116(8)	0.64(3)
C(25)	0.027(9)	0.19(1)	0.362(2)	0.24(7)	0.36
C(25)'	−0.004(2)	0.223(4)	0.3207(7)	0.114(9)	0.58(3)
C(26)	−0.056(3)	0.313(6)	0.334(1)	0.16(2)	0.42
C(26)'	−0.059(2)	0.304(4)	0.2936(7)	0.13(1)	0.58(5)
C(27)	−0.002(4)	0.234(6)	0.301(1)	0.12(2)	0.42
C(27)'	−0.009(2)	0.230(3)	0.2647(7)	0.111(8)	0.65(5)
C(28)	−0.055(4)	0.302(6)	0.273(1)	0.12(2)	0.35
C(28)'	−0.068(3)	0.307(4)	0.2345(8)	0.14(1)	0.59(4)
C(29)	−0.008(4)	0.239(6)	0.244(1)	0.12(1)	0.41
C(29)'	−0.005(2)	0.224(3)	0.2074(7)	0.102(9)	0.57(6)
C(210)	−0.044(4)	0.287(7)	0.215(1)	0.13(2)	0.43
C(210)'	−0.059(2)	0.305(4)	0.1803(8)	0.127(9)	0.58(3)
C(211)	0.013(4)	0.229(6)	0.187(1)	0.14(1)	0.42
C(211)'	0.002(3)	0.224(4)	0.1517(8)	0.14(1)	0.70(6)
C(212)	−0.044(5)	0.289(7)	0.160(1)	0.09(2)	0.30
C(212)'	−0.061(2)	0.300(3)	0.1233(6)	0.141(9)	0.61(3)
C(213)	0.012(5)	0.224(8)	0.133(1)	0.18(2)	0.39
	−0.006(1)	0.236(2)	0.0981(4)	0.182(6)	

coordinates of N and C atoms were determined from successive Fourier maps. For the solution of phases V', coordinates of the Zn and Cl atoms found in phase IV were used. The structures were refined by the block-diagonal least-squares method. The minimized function was $\Sigma w(\Delta F)^2$ with $w = 1/\sigma^2(F)$. Anisotropic thermal parameters were refined for Zn, Cl and N atoms and isotropic thermal parameters for C atoms. Final values of R, R_w and goodness of fit for the different phases are summarized in Table II. Atomic parameters of phases IV and V' are given in Tables III and IV respectively. Tables of anisotropic thermal parameters for Zn and Cl atoms, interatomic distances and structure factors are given as supplementary material.

The room temperature structure previously reported[7] consists of two types of alternating layers stacked along c. One layer consists of isolated $ZnCl_4$ tetrahedra whereas the other is formed by intercalated alkylammonium chains with their axis roughly parallel to the normal of the layer. The NH_3 groups of the aliphatic chains are fixed in the Cl-cavities by N-H. . .Cl hydrogen bonds. A projection of this structure along b is given in Figure 2. The cell contains four independent chains ($N1$, $N2$, $N3$ and $N4$) which are parallel to the (ac) plane but slightly inclined relative to the layer normal. Two of them ($N1$ and $N3$) are in the all-trans conformation whereas the other two ($N2$ and $N4$) have torsion angles of $-75°$ and $73°$ between $C(23)-C(24)$ and $C(42)-C(43)$ respectively. This optimizes the packing density of the aliphatic chains. One of the chains ($N4$) is somewhat disordered even at room temperature, especially in the area surrounding the two carbon atoms closest to the ammonium end.

In the high temperature phase, increases in the thermal motion of the carbon atoms and important changes in their torsion angles can be observed. These angles are reported on Table V along with the torsion angles of the room temperature phase. Structural changes are also observed in the inorganic layer where the tetrahedra are slightly shifted.

As expected from the DSC results, the most important structural change is observed in the first pre-transition V-IV. The chains reorient in a direction parallel to the layer normal and the two independent chains adopt the all-trans conformation (Table V). Figure 3 shows a projection of the structure of phase IV; a comparison of the two conformational states of chain $N4$ in V and IV is given in Figure 4.

In the following transitions, new conformational states appear in the aliphatic chains as derived from preliminary refinements of phase III and II.[13] In phase III, four independent chains coexist, two of which ($N3$ and $N4$), show torsion angles of $-72°$ and $87°$ respectively.

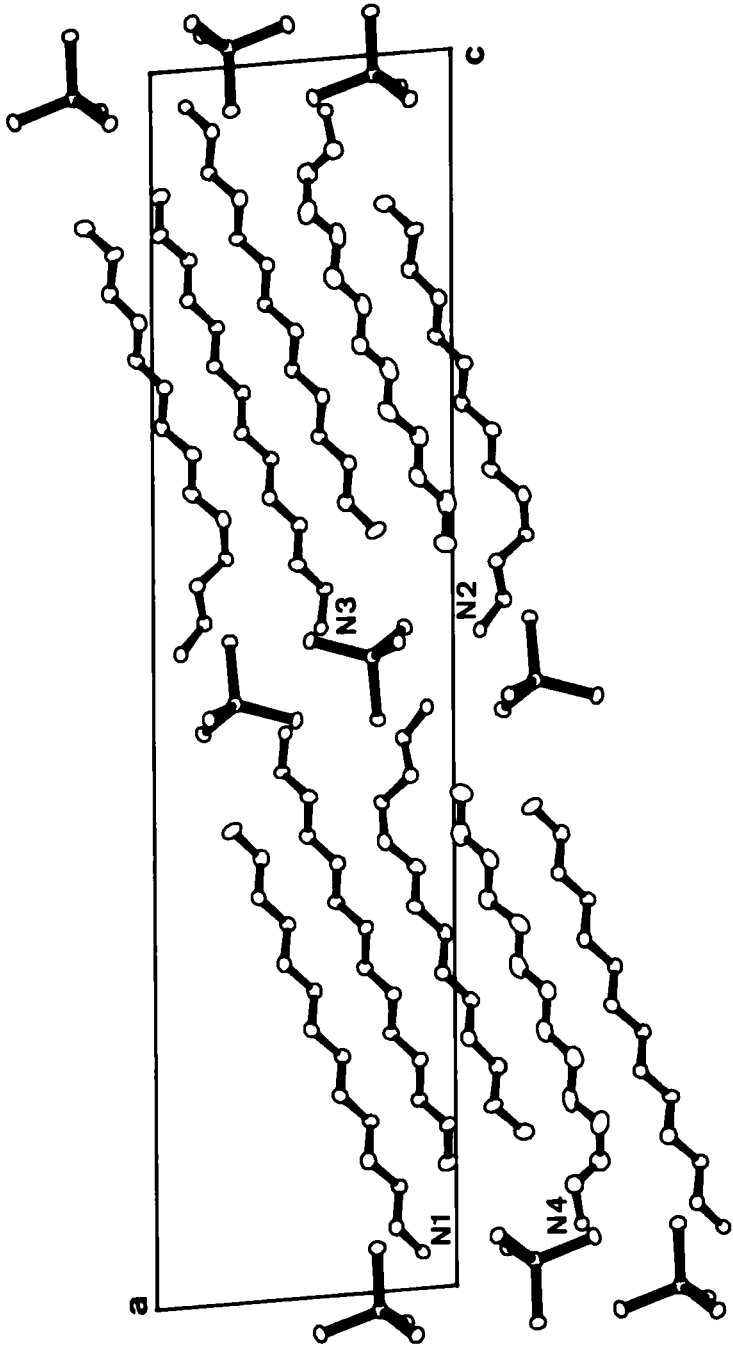

FIGURE 2 Projection along **b** of the room temperature phase of C13Zn (phase V). Atoms are represented with 20% thermal ellipsoids. The **a** + **c** diagonal represents the **c** axis of phase IV. The disorder in chain N4 is not shown.

TABLE V

Torsion angles of the aliphatic chains. Values of the room temperature phase (V) are also reported.

	V	IV	V′	
N(1) - C(11) - C(12) - C(13)	174(1)	176(2)	175(1)	
C(11) - C(12) - C(13) - C(14)	180(1)	174(2)	174(1)	
C(12) - C(13) - C(14) - C(15)	179(1)	−177(2)	−176(1)	
C(13) - C(14) - C(15) - C(16)	−177(1)	177(2)	176(1)	
C(14) - C(15) - C(16) - C(17)	180(1)	−179(2)	179(2)	
C(15) - C(16) - C(17) - C(18)	178(1)	178(2)	177(2)	
C(16) - C(17) - C(18) - C(19)	179(1)	180(2)	180(2)	
C(17) - C(18) - C(19) - C(110)	−179(1)	179(2)	178(2)	
C(18) - C(19) - C(110) - C(111)	−178(1)	179(2)	180(2)	
C(19) - C(110) - C(111) - C(112)	180(1)	179(2)	180(2)	
C(110) - C(111) - C(112) - C(113)	179(1)	178(2)	178(2)	
N(2) - C(21) - C(22) - C(23)	170(1)	177(3)	173(2)	−160(6)
C(21) - C(22) - C(23) - C(24)	−175(1)	176(3)	170(4)	− 32(8)
C(22) - C(23) - C(24) - C(25)	− 75(1)	165(3)	175(3)	−175(7)
C(23) - C(24) - C(25) - C(26)	−175(1)	−179(3)	−174(4)	171(4)
C(24) - C(25) - C(26) - C(27)	175(1)	177(3)	174(3)	177(5)
C(25) - C(26) - C(27) - C(28)	−178(1)	−179(3)	178(3)	179(5)
C(26) - C(27) - C(28) - C(29)	179(1)	178(3)	178(3)	−179(6)
C(27) - C(28) - C(29) - C(210)	179(1)	178(3)	−178(3)	175(6)
C(28) - C(29) - C(210) - C(211)	180(1)	179(3)	180(3)	177(6)
C(29) - C(210) - C(211) - C(212)	−179(1)	178(3)	176(3)	−178(6)
C(210) - C(211) - C(212) - C(213)	179(1)	180(4)	178(3)	179(6)
N(3) - C(31) - C(32) - C(33)	−177(1)			
C(31) - C(32) - C(33) - C(34)	177(1)			
C(32) - C(33) - C(34) - C(35)	−177(1)			
C(33) - C(34) - C(35) - C(36)	180(1)			
C(34) - C(35) - C(36) - C(37)	178(1)			
C(35) - C(36) - C(37) - C(38)	180(1)			
C(36) - C(37) - C(38) - C(39)	180(1)			
C(37) - C(38) - C(39) - C(310)	−179(1)			
C(38) - C(39) - C(310) - C(311)	−179(1)			
C(39) - C(310) - C(311) - C(312)	179(1)			
C(310) - C(311) - C(312) - C(313)	−177(1)			
N(4) - C(41) - C(42) - C(43)	168(2)			
N(4) - C(41)′ - C(42)′ - C(43)	−157(3)			
C(41) - C(42) - C(43) - C(44)	73(2)			
C(41)′ - C(42)′ - C(43) - C(44)	− 89(2)			
C(42) - C(43) - C(44) - C(45)	155(2)			
C(42)′ - C(43) - C(44) - C(45)	−155(2)			
C(43) - C(44) - C(45) - C(46)	179(2)			
C(44) - C(45) - C(46) - C(47)	176(2)			
C(45) - C(46) - C(47) - C(48)	−178(2)			
C(46) - C(47) - C(48) - C(49)	178(2)			
C(47) - C(48) - C(49) - C(410)	180(2)			
C(48) - C(49) - C(410) - C(411)	180(2)			
C(49) - C(410) - C(411) - C(412)	180(2)			
C(410) - C(411) - C(412) - C(413)	−177(2)			

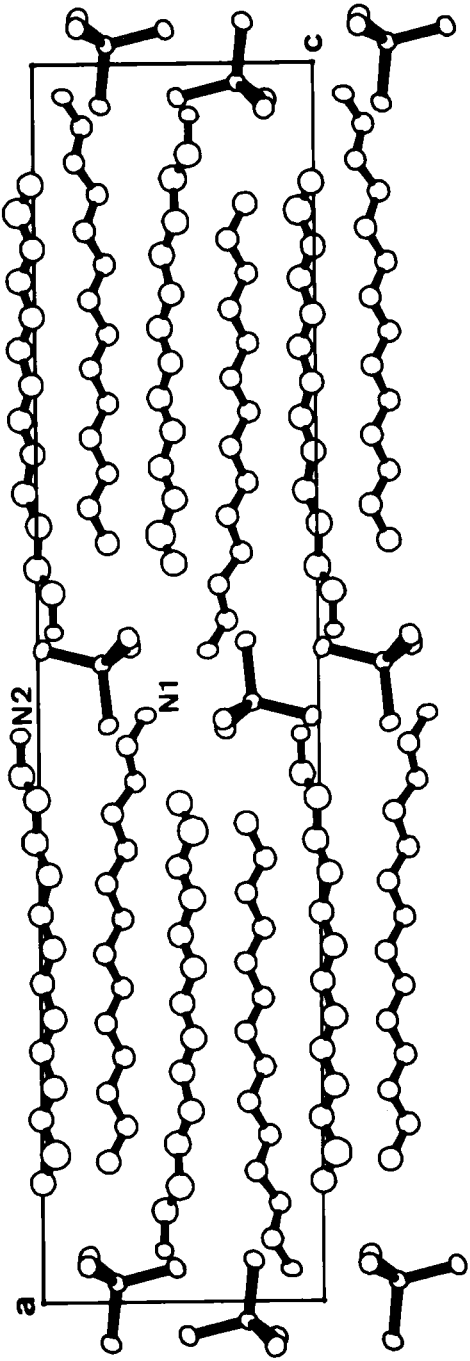

FIGURE 3 Projection of phase IV along **b**. N1 and N2 indicate nitrogen atoms of the two independent chains as given in Table III. Atoms are represented with 20% thermal ellipsoids.

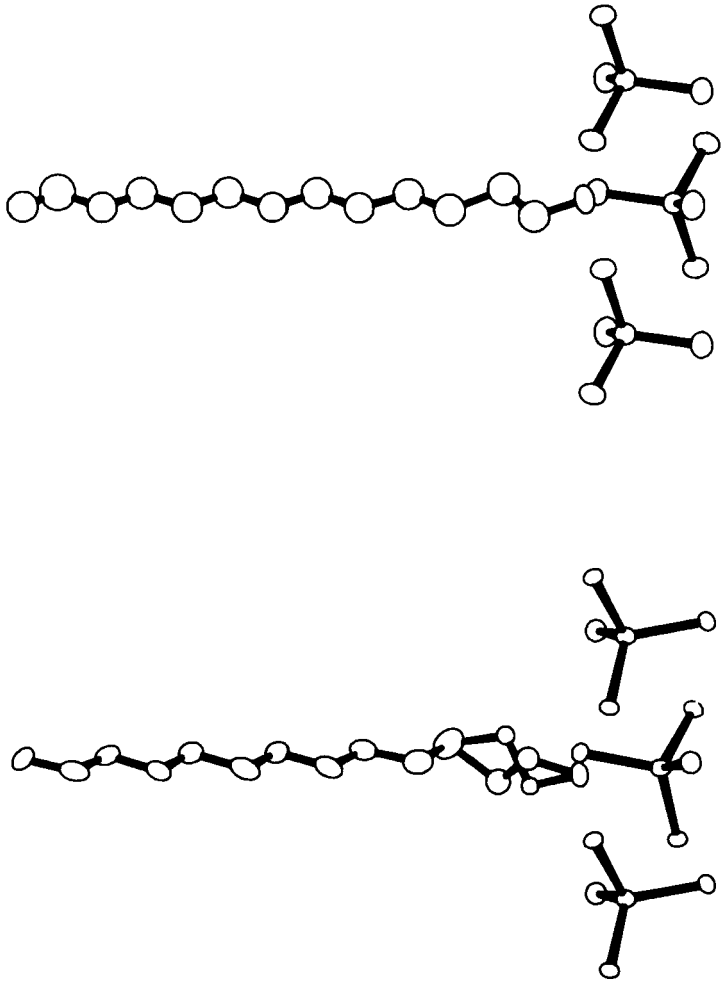

FIGURE 4 Comparison of the same chain before the transition (phase V, left) and after (phase IV, right). Anisotropic and isotropic thermal parameters are represented for phase V resp. phase IV with 20% thermal ellipsoids. The disordered part of chain N4 in phase V is represented by the two partially populated atomic positions.

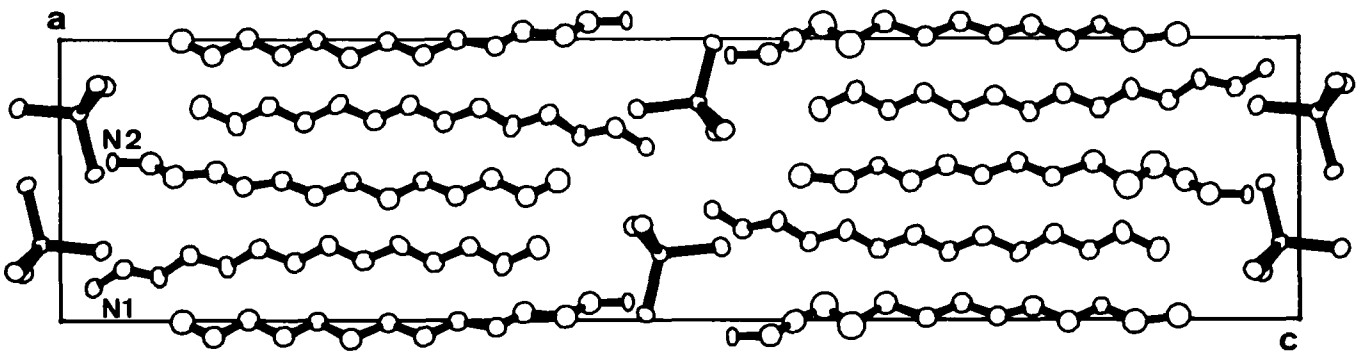

FIGURE 5 Projection of phase V′ along **b** with 20% thermal ellipsoids. For clarity, only one unit of the disordered chain (N2) has been represented on the figure.

In addition, the $N3$ chains exhibit two disordered carbon atoms near the ammonium end which can be interpreted as an additional conformation with a torsion angle of 167°. Other important torsion angles up to 144° appear at various positions in the chains.

The structure of phase V′ (Figure 5) is similar to phase IV but with an additional disorder: the $N2$-chain was refined with carbon atoms ($C23$ to $C213$) distributed among two positions. Individual atomic population parameters were refined yielding an average value of 0.6 for one chain and 0.4 for the other. This disorder must be interpreted as static rather than dynamic owing to the large distance between the two chains. One chain is similar to the $N2$ chain in phase IV whereas the other has a torsion angle of $-32°$ about the $C(22)-C(23)$ bond. This value is very inaccurate since the position of $C(22)$, refined as a single position is very uncertain.

4. DISCUSSION

The structural information for the various phases gives an important insight into the mechanisms of the transitions. Finding four independent chains in phase V is an interesting observation. Obviously, the tendency for each chain to acquire the all-trans conformation can only be satisfied for two of them. The two additional crystallographically independent chains introduce a "kink" each on a different carbon atom near the ammonium end. Another characteristic feature of this phase concerns the systematically higher thermal ellipsoids of one single chain (chain 4) relative to the other three. The *n*-alkylammonium layer is thus divided in domains of alternating chain densities rather than the disorder being spread uniformly on the four independent chains.

The V to VI transition is accompanied by the disappearance of all the kinks; the largest deviation from the all-trans conformation in the torsion angles of the two independent chains is 15°. Figure 4 shows for example one of the chains ($N4$, phase V) below and above ($N2$, phase IV) the transition at 304 K. The chains are related by a rotation of approximately 180° about the chain axis. In addition, the vertical axis of the chain has shifted relative to the layer of the $ZnCl_4$ tetrahedra in direction of the b axis. As a result of the two types of displacements, the kink observed in the room-temperature phase on the second and third *C*-atoms has disappeared in the first high temperature phase. The other crystallographically independent chain ($N3$, phase V) which transforms into chain $N2$ (phase IV) can be match

by a rotation of approximately 90° about the chain axis combined to a parallel displacement in the direction of *b* but opposite to the corresponding displacement of chain *N*4. For the other two independent chains (*N*1, *N*2) similar displacements can be observed. The disappearance of the kink on chain *N*2 at higher temperature is again accompanied by a rotation of 180° about the chain axis and a parallel displacement of the chain along *a*. The displacements of chains *N*2 and *N*3 are comparable. Figure 3 shows that the tendency to acquire the all-trans conformation for all chains could only be satisfied by the introduction of a slight bent of the chains near the ammonium end. It is very probable that the bent on the chains will disappear in phase III.

The structural transition V to IV can also be interpreted as the result of a shear strain perpendicular to the *b* axis. In this transition, the monoclinic angle β increases from 94° to 100°. The transition from IV to III results from another shear strain but perpendicular to the *a*-axis with an increase of α by 3.4°.

All the transitions are reversible with the exception of the phase V to IV transition. Phase V can no longer be observed after a heating cycle. Instead, phase V′ is stable at room-temperature; phase V must therefore be considered to be metastable. The structure of phase V′ can be interpreted as consisting of four chains, by taking the disorder into account, three of which with the all-trans conformation. Obviously, phase V′ is more stable with three out of four chains in this conformation instead of the 2/2 ratio observed in phase V.

The sequence of structures of the various phases shows a very interesting example of the dynamics of the alkyl chains. The stability of some chain conformations is often limited to a narrow temperature interval. The periodicity constraints which are imposed on the system of chains by the $ZnCl_4$ tetrahedra plays certainly an important role in the sequence of phase transitions. The array of hydrogen bonds between the Cl and the N atoms acts as a semirigid framework on which the polar ends of the chains are attached and therefore introduces constraints to the system. The sequence of structural phase transitions can thus be considered as a series of steps towards their total release by increasing temperature.

References

1. C. Socias, M. A. Arriandiaga, M. J. Tello, J. Fernandez and P. Gili, *Phys. Stat. Sol.*, **(a) 57**, 405 (1980).
2. R. Blinč, M. Koželj, V. Rutar, I. Zupančič, B. Žekš, H. Arend, R. Kind and G. Chapuis, *Faraday Discuss. Chem. Soc. No. 69*, **58** (1980).

3. R. Kind, S. Pleško, H. Arend, R. Blinč, B. Žekš, J. Seliger, B. Ložar, J. Slak, A. Levstik, C. Filipič, V. Žagar, G. Lahajnar, F. Milia and G. Chapuis, *J. Chem. Phys.*, **71**, 2118 (1979).
4. M. Koželj, V. Rutar, I. Zupančič, R. Blinč, H. Arend, R. Kind and G. Chapuis, *J. Chem. Phys.*, **74**, 4123 (1981).
5. J. Fernandez, C. Socias, M. A. Arriandiaga, M. J. Tello and A. Lopez Echarri, *J. Phys. C.*, **15**, 1151 (1982).
6. F. J. Zuñiga and G. Chapuis, *Cryst. Struct. Commun.*, **10**, 533 (1981).
7. F. J. Zuñiga and G. Chapuis, *Acta Cryst.*, **B39**, 620 (1983).
8. C. Socias, Doctoral Thesis, Univ. Pais Vasco, Bilbao, Spain. (1980).
9. The X-ray System—version of June 1972. Tech. Rep. TR-192. Computer Science Center, Univ. of Maryland, College Park, Maryland, USA.
10. D. T. Cromer and J. B. Mann, *Acta Cryst.*, **A24**, 321 (1968).
11. D. T. Cromer and D. Liberman, *J. Chem. Phys.*, **53**, 1891 (1970).
12. K. J. Schenk, PhD Thesis, Univ. of Lausanne (1984).
13. F. J. Zuñiga and G. Chapuis. To be published.